# Supporting Information

# The redox kinetics of the amyloid-β-Cu complex and its biological implications

Paul Girvan,[†§] Xiangyu Teng,[†] Nicholas J. Brooks,[†§] Geoffrey S. Baldwin,[§‡] and Liming Ying[§#]

[†]Department of Chemistry, [§]Institute of Chemical Biology, [‡]Department of Life Sciences, [#]National Heart & Lung Institute, Imperial College London, London, United Kingdom.

## Materials

HEPES (4-(2-Hydroxyethyl)-1-piperazineethanesulfonic acid) purchased from Sigma-Aldrich (UK) as a pH 7.5 buffered solution was used throughout this work. Milli-Q$^{TM}$ 'ultrapure' water with a resistivity of 18.2 MΩ cm was used throughout. Sodium chloride (NaCl) (Sigma-Aldrich, UK) at a purity ≥ 99.5 % was dissolved in Milli-Q$^{TM}$ water to create a 2 M stock solution which was stored at 5 °C. Copper(II) chloride dihydrate ($CuCl_2$) at a purity > 99 % was purchased from Sigma-Aldrich (UK) and dissolved in water to create a 20 mM stock solution which was stored at 5 °C. Ascorbate solutions were made immediately prior to each experiment (to minimize auto-oxidation) by dissolving (+)-sodium L-ascorbate (Sigma-Aldrich, UK) ≥ 99.0 % in 50 mM HEPES (pH 7.5) buffer containing 100 mM NaCl. Hydrogen peroxide ($H_2O_2$) solutions were prepared by diluting a 35 wt. % hydrogen peroxide solution (Sigma-Aldrich, UK) in 50 mM HEPES (pH 7.5) buffer containing 100 mM NaCl. The amyloid-β peptides used in this work (except for A2P-Aβ) were all purchased labeled with HiLyte$^{TM}$ Fluor 488 on either the Lys16 for Aβ16 or in the case of Aβ40 at a cysteine that was introduced at position 20. All peptides (except for A2P-Aβ) were purchased from AnaSpec (CA, USA) via Cambridge Bioscience (UK). The A2P-Aβ sample was purchased labeled with fluorescein isothiocyanate (FITC) on Lys16, and obtained from SynPeptide (China). The Aβ16 peptides were dissolved in 50 mM HEPES (pH 7.5) buffer containing 100 mM NaCl and stored at −20 °C. The Aβ40 peptide was dissolved in 1 % ammonium solution (to prevent it from aggregating) and stored at −20 °C. The concentration of stock solutions was determined using a UV/Vis Spectrometer (Lambda 25, PerkinElmer, MA, USA) and using an extinction coefficient for the peak absorbance of the dye (ε= 70 000 $cm^{-1}$ $M^{-1}$ for HiLyte$^{TM}$ Fluor 488 and ε= 73 000 $cm^{-1}$ $M^{-1}$ for FITC). Peptides were diluted to required concentrations in 50 mM HEPES (pH 7.5) buffer containing 100 mM NaC immediately prior to use.

### Peptides used in this work

| | | | | | | | | | |
|---|---|---|---|---|---|---|---|---|---|
| Aβ16 | DAEFR | HDSGY | EVHHQ | K* | | | | | |
| mAβ | DAEFG | HDSGF | EVRHQ | K* | | | | | |
| A2P-Aβ | DPEFR | HDSGY | EVHHQ | K* | | | | | |
| Aβ16(H6R) | DAEFR | RDSGY | EVHHQ | K* | | | | | |
| Aβ40 | DAEFR | HDSGY | EVHHQ | KLVFC* | AEDVG | SNKGA | IIGLM | VGGVV | |
| | * HiLyte 488 | | * FITC | | | | | | |

## Fluorometer measurements

Steady state fluorescent measurements were made using a FluoroMax®-4 (HORIBA) fluorometer. In all cases the excitation and emission wavelengths were set to 488 nm & 525 nm respectively. Excitation and emission slit widths were chosen such that the fluorescent intensity was ca. $10^4$-$10^5$ counts per second to remain well within the linear range of the instrument. Integration time for each point was set to 1 s.

## Correction of quenching due to ascorbate ion

At high concentrations of ascorbate, a quenching of the fluorescence from the HiLyte488 labeled amyloid beta peptide was noted. To correct for this a Stern-Volmer analysis was carried out via Eq.1

$$\frac{I_f^0}{I_f} = 1 + k_q \tau_0 \cdot [Q] \tag{1}$$

where $I_f^0$ is the fluorescence intensity in the absence of quencher, $I_f$ is the intensity in the presence of quencher, $k_q$ is rate constant of the quenching process, $\tau_0$ is the fluorescence lifetime of the dye and [Q] is the concentration of quencher used.

From this, a plot of $I_f^0/I_f$ against [Q] should yield a straight line plot, the fitting of which can be used to correct for quenching due to the ascorbate added (Fig. S1).

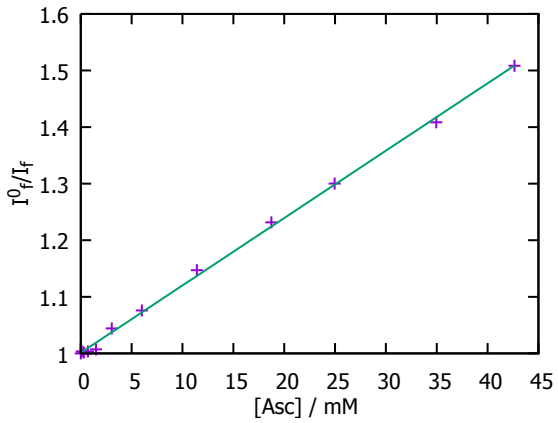


**Figure S1** Stern-Volmer plot of quenching of HiLyte488 labeled amyloid beta with ascorbate.

The correction used thought all this work is given in Eq.2.

$$\frac{I_f^0}{I_f} = 1.001(3) + 11.9(1) \cdot \text{molar ascorbate concentration} \tag{2}$$

## Stopped flow

A KinetAsyst SF-610X2 stopped flow spectrophotometer (HI-TECH Scientific, UK) was used for the kinetic measurements in this work. All experiments were performed at 298 K. The buffer system for all experiments was comprised of HEPES (50 mM) pH 7.5, containing NaCl (100 mM). Samples were excited using a fiber coupled laser diode (MCLS1-473-20, Thorlabs, CA, USA) at 473 nm. Fluorescence emission was filtered using a 515 nm long pass filter (515GY, Comar, UK) before being detected by a photon multiplier tube. Data points were taken using a log time-scale sampling scheme. For each data point, a minimum of 7 traces were averaged. Time points below 2 ms were excluded due to the instrument dead time (∼1 ms). The raw curves were fitted with exponentials using OriginPro 2015 (OriginLab, USA). All error bars shown represent the uncertainty of the fits of the raw data.

### Single mixing reduction kinetics

Apart from where explicitly stated otherwise, single mixing reduction kinetics were carried out using the human Aβ16 peptide. A syringe containing AβCu(II) was rapidly mixed with a second syringe containing various concentrations of ascorbate. During mixing the concentration of each solution is halved, resulting in a final concentration detailed in the captions and figure legends of the relevant figures. The increase in fluorescence is recorded.

### Double mixing reduction kinetics

For the double mixing reduction experiments (Fig. 3C and 3D in the main text) we are able to probe the reduction of freshly formed AβCu(II) as it goes from initially being all in the Component I conformation until it interconverts to Component II and eventually reaches equilibrium. This is carried out by originally having Aβ in one syringe and Cu(II) in a second syringe. These solutions are rapidly mixed (1:1 volume dilution) to give final concentrations after the first mixing of 50 nM Aβ, 1 µM Cu. This concentration of copper was chosen so that the binding to Aβ would be rapid and complete within the dead time of the instrument, such that before the 2nd mixing with ascorbate occurs all of the Aβ is present as AβCu(II). While it has been reported that Aβ can bind multiple Cu(II) ions[1] the 2nd copper binds much more weakly to Aβ[2][3] and significantly slower than the first copper.[3] As we only record for ∼10 s we do not expect any 2nd copper binding to have occurred during our measurements. Finally, after a defined delay, that was varied between 100 ms and 5 s, the freshly formed AβCu(II) solution from the first mixing is mixed with a third syringe containing ascorbate. The increase in fluorescence is recorded.

### Double mixing oxidation kinetics

Initially AβCu(II) is reduced by mixing with ascorbate. After a delay of 5 s to allow the reduction process to complete, the newly formed AβCu(I) is re-oxidised by $H_2O_2$. The decrease in fluorescence is recorded.

In this study we use $H_2O_2$ as the oxidant to probe AβCu(I) oxidation. The concentration of oxygen was not controlled or measured in our buffers. We can assume that the oxygen concentration was that of air saturated water at 25 °C (∼200 µM). The rate constant for the oxidation of 'free' Cu(I) to C(II) by $O_2$ has been reported to be two orders of magnitude

slower than the rate constant of oxidation by $H_2O_2$.[4] While we would expect the oxidation of the AβCu(I) complex to be different from 'free' Cu(I), we assume that the trend is likely to be the same, i.e. the oxidation rate of AβCu(I) complex by $O_2$ is much slower than $H_2O_2$. We would therefore not expect any oxidation by dissolved $O_2$ to take place within the timescales of our stopped flow experiments.

## Reduction kinetics of Aβ40Cu(II) complex

In all the work described in the main text the Aβ peptide used was a truncated version of the full-length peptide consisting of the first 16 amino acids. To confirm that Aβ16 is an acceptable model for the full length peptide, the reduction of the Aβ40Cu(II) complex was also carried out (Fig. S2). In all of the traces it can be seen that the signal begins to decrease after ∼2 s. This decrease is present even in the traces for just Aβ40 and Aβ40Cu(II) alone (where no ascorbate is added) and so cannot be a process related to the reduction. We have ascribed this process to the Aβ40 peptide adsorbing to the surface of the stopped flow instrument. At the low concentrations at which we conduct out experiments (50 nM) peptide adsorption onto surfaces presents a major problem which is exacerbated by the hydrophobicity of the Aβ C-terminal tail. This adsorption is not observed in experiments performed with Aβ16.

At time scales below 2 s the traces show a similar biphasic trend that is observed for the Aβ16Cu(II) complex (Fig. 3A of the main text). The traces for the reduction of Aβ40Cu(II) were globally fit while sharing the rate of peptide adsorption across all fits. This allowed us to obtain the rates of the fast and slow phases (Fig. S2 right panel) which display a similar dependence on ascorbate concentration as was observed for the Aβ16Cu(II) complex.

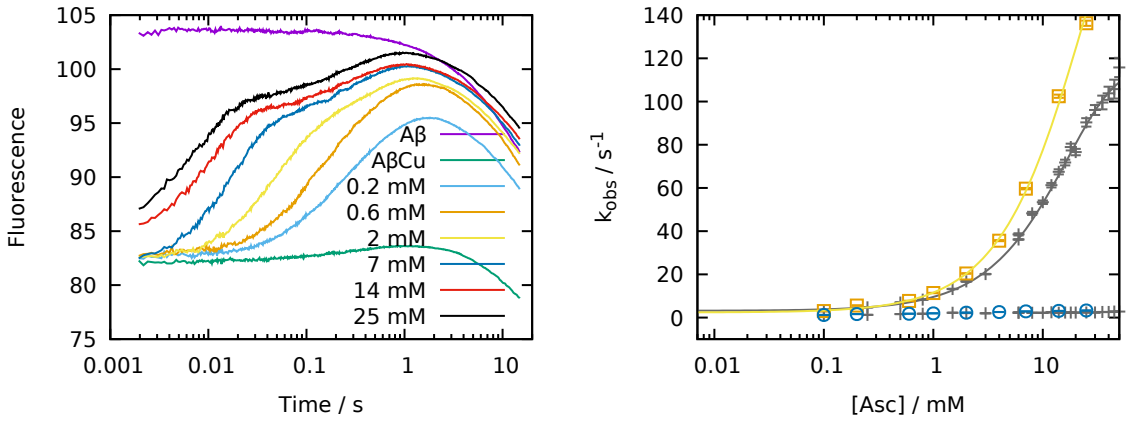


**Figure S2** Left panel: Stopped flow data showing the recovery of fluorescence after mixing 50 nM Aβ40Cu(II) with ascorbate (concentration given in key). Right panel: Rate of fast and slow phases determined from the exponential global fitting of the data shown in the left panel (sharing the rate of peptide adsorption across all traces). Data for the Aβ16 is shown in gray for comparison. Each kinetic trace represents the average of at least 7 repeats, error bars show the error of the fit. Experiments were performed at 298 K in HEPES buffer at pH 7.5

## Assignment of the fast and slow phases of reduction

Throughout the main text we ascribed the fast phase of the reduction experiments to the reduction of Component I and the slow phase to the interconversion of Component II to Component I and subsequent reduction. This assignment can be verified by using mutant Aβ peptides which differ in their p$K_a$.

The murine Aβ (mAβ) peptide contains three mutations compared to the human peptide, all of which occur within the metal binding region: Arg5Gly, Tyr10Phe & His13Arg. One of the key differences these mutations impart is a decrease in the p$K_a$ of the interconversion between Components I & II; human Aβ has a p$K_a$ of 7.7 while murine has a p$K_a$ of 6.2.[5] The result of this difference in p$K_a$ is that at physiological pH the equilibrium between Components I & II for human Aβ will lie slightly towards Component I, while mAβ will be almost exclusively in the Component II coordination.

Conversly, introducing an Ala2Pro mutation in human Aβ (A2P-Aβ) has been reported to shift the p$K_a$ from 7.7 to 8.8.[6] Therefore, at physiological pH the equilibrium between Components I & II for A2P-Aβ will be almost exclusively Component I.

As the relative proportions of Components I & II for mAβ and A2P-Aβ differ from human Aβ we would expect this to be reflected in the reduction kinetics. For mAβ the reduction will be dominated by the slow phase overserved with human Aβ, i.e. interconversion of Component II to Component I and subsequent reduction. In contrast, A2P-Aβ will be dominated by the fast phase observed with human Aβ. Fig. S3 shows how the rate of the dominate phases for mAβ and A2P-Aβ varies with ascorbate concentration. As expected the rate for mAβ matches the slow phase observed in Fig. 3A while the rate of A2P-Aβ matches the fast phase observed in Fig. 3A.

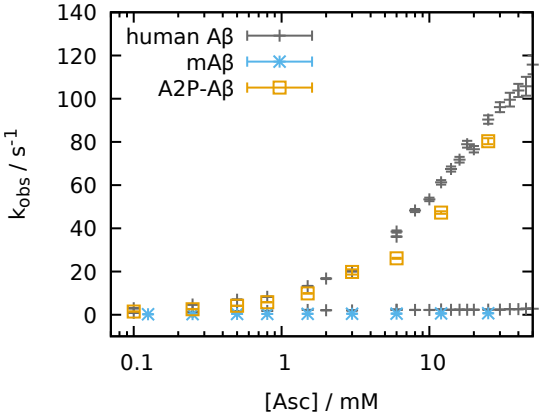


**Figure S3** Comparison of the reduction kinetics for human Aβ, mAβ and human Aβ with an A2P mutation (A2P-Aβ). Two phases were clearly resolved for human Aβ, while only one phase was dominant for both mAβ and A2P-Aβ. For A2P-Aβ the kinetics matches the fast phase of human Aβ, while for mAβ the kinetics matches the slow phase. Each kinetic trace represents the average of at least 7 repeats. Experiments were performed at 298 K at pH 7.5

## Reduction kinetics of H6R-AβCu(II) complex

The H6R substitution mutation, also known as the English mutation, is one of several mutations within the Aβ peptide that causes familial Alzheimer's disease. As the H6R-Aβ peptide lacks one of the histidine residues that coordinates to the metal center, a slightly different Cu(II) coordination environment has been described.[7] It has been reported that while the H6R mutation has little effect on the binding kinetics, the dissociation rate does differ, resulting in the Cu(II) being bound less tightly to the H6R-Aβ peptide.[8] Perhaps more importantly for the disease, it has also been shown that Cu(II) assisted dimerization is faster for the H6R mutant compared to the wild-type.[8] We set out to address if this H6R familial Alzheimer's disease mutation also has an impact on the ability of the peptide to produce reactive oxygen species by measuring the reduction kinetics (Fig. S4).

As can be seen in the right panel of Fig. S4, the H6R- and wild-type Aβ peptide have identical rates for the fast and slow phases. This shows that, somewhat surprisingly, the removal of one of the coordinating histidine ligands does not impact the rate of reduction. This result gives us a mechanistic insight into the nature of the reactive intermediate state, and suggests that histidine 6 is not involved. Our observation that removal of the coordinating histidine 6 residue does not affect the rate of reduction matches previous predictions for the coordination of the reactive intermediate state.[9]

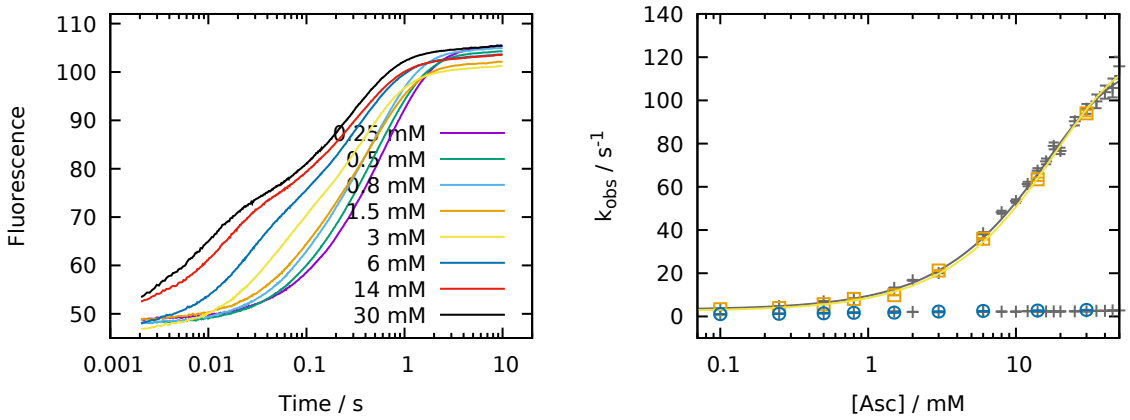


**Figure S4** Left panel: Stopped flow data showing the recovery of fluorescence after mixing 50 nM H6R-AβCu(II) with ascorbate (concentration given in key). Right panel: Rate of fast and slow phases determined from the exponential fitting of the data shown in the left panel. Data for the wild-type Aβ is shown in gray for comparison. Each kinetic trace represents the average of at least 7 repeats, error bars show the error of the fit. Experiments were performed at 298 K in HEPES buffer at pH 7.5

## Oxidation control experiments

As explained in the main text the oxidation experiments are carried out under conditions where there is excess ascorbate also present, and so we only use the initial rate when determining the rate constant of oxidation. The initial rate should be independent of ascorbate as at very short timescales no reduction would be able to take place. The left panel of Fig. S5 shows that the initial rate of oxidation is independent of ascorbate concentration. The obtained rate constants are within error of each other at two very different ascorbate concentrations, $4.3(2) \times 10^2\,\mathrm{M}^{-1}\,\mathrm{s}^{-1}$ and $4.4(2) \times 10^2\,\mathrm{M}^{-1}\,\mathrm{s}^{-1}$.

The right panel of Fig. S5 shows control experiments that were carried out to ensure that fluorescent changes observed were not due to oxidative damage of the HiLyte$^{\mathrm{TM}}$ Fluor 488 dye. Even under $H_2O_2$ concentrations and recording times vastly exceeding what were used, fluorescence decrease due to direct oxidation of the fluorophore is negligible.

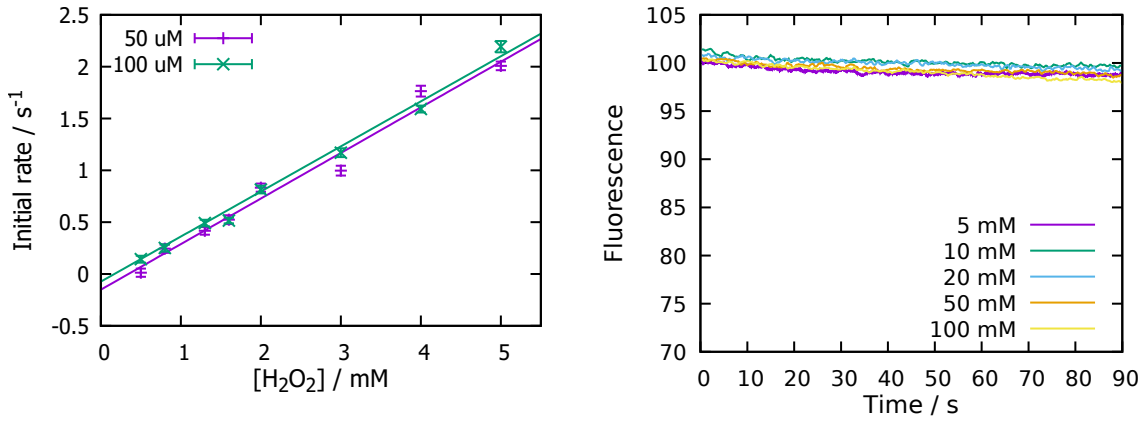


**Figure S5** Left panel: Initial rate of AβCu(I) oxidation is independent of the concentration of ascorbate used to prepare the AβCu(I) (concentration given in key). Right panel: Stopped flow data showing the change in fluorescence after mixing 50 nM Aβ with $H_2O_2$ concentrations $\geq$ to what were used in this study. Concentration of $H_2O_2$ given in key. The fluorescent dye was only appreciably damaged when concentrations vastly higher and timescales much longer than what were employed in this study were used. Experiments were performed at 298 K in HEPES buffer at pH 7.5

## References


1. B. Alies, E. Renaglia, M. Rózga, W. Bal, P. Faller, and C. Hureau, Cu(II) Affinity for the Alzheimer's Peptide: Tyrosine Fluorescence Studies Revisited *Anal. Chem.*, **85** (3), 1501-1508, (2013).

2. L. Guilloreau, L. Damian, Y. Coppel, H. Mazarguil, M. Winterhalter and P. Faller, Structural and thermodynamical properties of CuII amyloid-β16/28 complexes associated with Alzheimer's disease *J. Biol. Inorg. Chem.*, **11**, 1024 (2006).

3. T. Branch, M. Barahona, C. A. Dodson, and L. Ying, Kinetic Analysis Reveals the Identity of Aβ-Metal Complex Responsible for the Initial Aggregation of Aβ in the Synapse *ACS Chemical Neuroscience*, **8**, 1970-1979, (2017).

4. N. Pérez-Almeida, M. González-Dávila, J. M. Santana-Casiano, A. G. González, and M. Suárez de Tangil, Oxidation of Cu (I) in seawater at low oxygen concentrations, *Environ. Sci. Technol.* **47**, 1239-1247, (2013).

5. H. Eury, B. C. Bijani, P. Faller, and C. Hureau, Copper (II) coordination to amyloid β: murine versus human peptide, *Angew. Chem. Int. Ed.*, **50**, 901-905 (2011).

6. N. Yako , T. R. Young , J. M. Cottam Jones , C. A. Hutton , A. G. Wedd and Z. Xiao, Copper binding and redox chemistry of the Aβ16 peptide and its variants: insights into determinants of copper-dependent reactivity, *Metalomics*, **9**, 278-291, (2017).

7. B. Alies, H. Eury, C. Bijani, L. Rechignat, P. Faller, and C. Hureau, pH-Dependent Cu(II) Coordination to Amyloid-β Peptide: Impact of Sequence Alterations, Including the H6R and D7N Familial Mutations, *Inorg. Chem.*, **50**, 11192-11201, (2011).

8. P. Girvan, T. Miyake, X. Teng, T. Branch, and L. Ying, Kinetics of the Interaction between Copper and Amyloid-β with FAD Mutations and Phosphorylation at the N terminus, *ChemBioChem*, **17**, 1732-1737, (2016).

9. L. Cassagnes, , V. Hervé, F. Nepveu, C. Hureau, P. Faller, and F. Collin, The Catalytically Active Copper-Amyloid-Beta State: Coordination Site Responsible for Reactive Oxygen Species Production, *Angew. Chem. Int. Ed.*, **52**, 11110-11113, (2013).